

Sol–Gel Processes

A Natural Glycyrrhizic Acid-Tailored Light-Responsive Gelator

Heshu Fang,^[a, c] Xia Zhao,^[c] Yuan Lin,^[c] Song Yang,^{*,[a]} and Jun Hu^{*,[b, c]}

Abstract: The construction of stimuli-responsive materials by using naturally occurring molecules as building blocks has received increasing attention owing to their bioavailability, biocompatibility, and biodegradability. Herein, a symmetrical azobenzene-functionalized natural glycyrrhizic acid (*trans*-GAG) was synthesized and could form stable supramolecular gels in DMSO/H₂O and MeOH/H₂O. Owing to *trans*–*cis* isomerization, this gel exhibited typical light-re-

sponsive behavior that led to a reversible gel–sol transition accompanied by a variation in morphology and rheology. Additionally, this *trans*-GAG gel displayed a distinct injectable self-healing property and outstanding biocompatibility. This work provides a simple yet rational strategy to fabricate stimuli-responsive materials from naturally occurring, eco-friendly molecules.

Introduction

Low-molecular-weight gels (LMWGs), or supramolecular gels, which arise from the self-assembly of small molecules into 3D networks to immobilize solvents, are a fascinating class of materials.^[1] Compared with traditional polymer gels, the properties of LMWGs can be reversibly tuned by the input of chemical or physical stimuli, such as pH,^[2] ultrasound,^[3] light,^[4] ligands,^[5] enzymes,^[6] and mechanical force.^[7] Of these, light has attracted immense attention because it is a fast and non-contaminating stimulus that can provide a broad range of tunable parameters, for example, wavelength, intensity, and duration.^[1d,8] By incorporating light-active moieties (diarylethene, spiropyran, azobenzene) into the gelator, the microstructure of LMWGs can be manipulated easily upon exposure to light.^[9] For example, Nilsson and co-workers have fabricated a light-sensitive azobenzene–peptide hydrogel that showed a reversible sol–gel transition induced by UV/Vis light, which thus allowed the light-triggered release of encapsulated pharmaceuti-

cal agents.^[10] Liu et al. found that the curvature of protein nanowires could be alternated by using a light-isomerizable azobenzene-cored poly(amidoamine) (PAMAM) dendrimer evoked SP1 (stable protein 1) protein assembly, which offers a potential strategy for the design of intelligent protein-based nanobiomaterials.^[9a] Obviously, although light-responsive LMWGs have been around for many years, they are still receiving considerable current interest.

Glycyrrhizic acid (**GA**, Scheme 1), a natural triterpenoid saponin mainly found in licorice root, is widely used in candies and sweets on account of its intense sweetness^[11] and exhibits many biological activities, such as antitumor, anti-inflammatory, antiviral, and antibacterial effects.^[12] From a structural point of view, **GA** is comprised of a hydrophobic triterpenoid aglycon moiety (glycyrrhetic acid) and a hydrophilic diglucuronic unit, which endows it with a classic amphiphilic nature. In 2015, Mezzenga et al. first reported its fibrillar self-assembled features in the preparation of Au nanoparticle–hybrid gels.^[13] Next, Yang and co-workers used **GA** to fabricate plant-oil-structured emulsion gels.^[14] To date, only four works on **GA** gels have been reported,^[13,14] and the combination of **GA** with functional units to afford responsive LMWGs is still rare.

[a] H. Fang, Dr. S. Yang

State Key Laboratory Breeding Base of Green Pesticide & Agricultural Bioengineering, Centre for R&D of Fine Chemicals
Guizhou University
Guiyang 550025 (China)
E-mail: yangsdqj@126.com

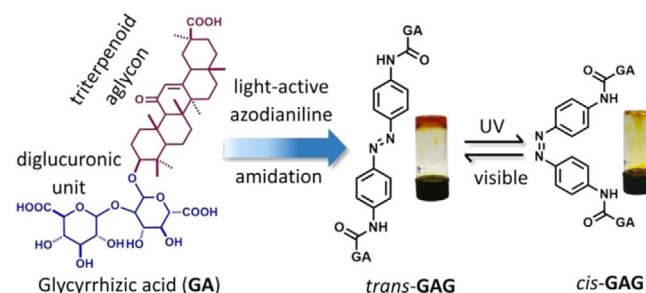
[b] Dr. J. Hu

Beijing Advanced Innovation Center for Soft Matter Science and Engineering, Beijing University of Chemical Technology
Beijing 100029 (China)
E-mail: jhu@mail.buct.edu.cn

[c] H. Fang, Dr. X. Zhao, Dr. Y. Lin, Dr. J. Hu

State Key Lab of Polymer Physics and Chemistry
Changchun Institute of Applied Chemistry
Chinese Academy of Sciences
Changchun 130022 (China)

Supporting information and the ORCID identification number(s) for the author(s) of this article can be found under <https://doi.org/10.1002/asia.201800180>.



Scheme 1. Schematic representation of the gelation of *trans*-GAG and its reversible *trans*–*cis* isomerization.

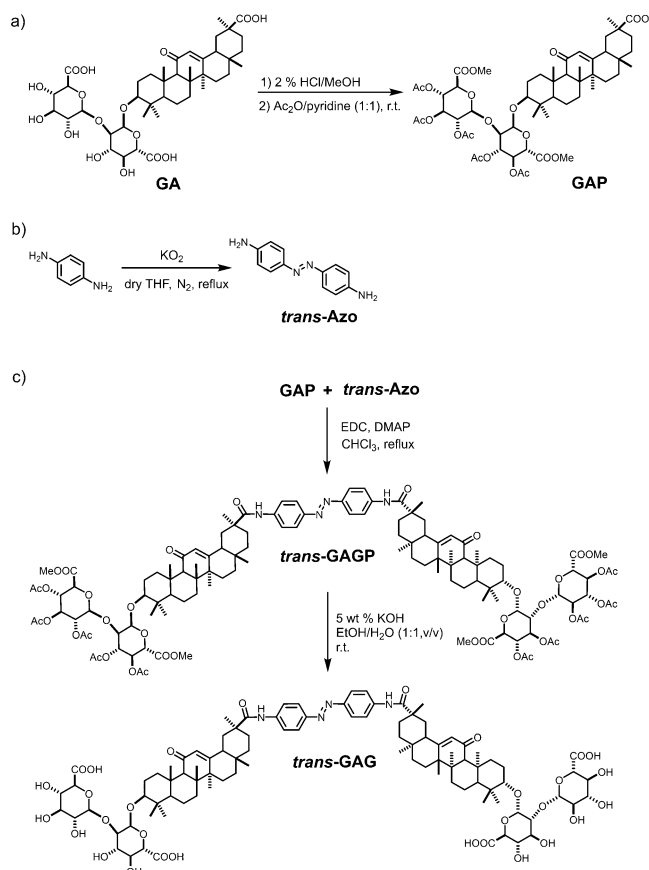
Herein, a symmetrical molecule, *trans*-GAG, in which two natural GA moieties are linked by an azobenzene group through the amide bond, was designed and synthesized as shown in Scheme 1. In this molecule, the azobenzene chromophore can participate in an efficient, reversible *trans*-*cis* isomerization, whereas GA supplies the amphiphilic backbone to form LMWGs. Furthermore, naturally occurring GA has good bioavailability, biocompatibility, and biodegradability, which endow it with potential applications in the field of biomedicine. The results showed that *trans*-GAG formed supramolecular gels in DMSO/H₂O and MeOH/H₂O. Upon irradiation with alternating UV and visible light, it underwent a reversible *cis*-GAG/*trans*-GAG isomerization, which thus resulted in gel-sol transitions accompanied by a variation in morphology and rheology. Additionally, the *trans*-GAG gel exhibited a distinct injectable self-healing property and outstanding biocompatibility, which provides a way to fabricate natural-product-containing stimuli-responsive biomaterials for potential drug release and 3D printing.

Results and Discussion

GA is a polyprotic weak acid and its dissociation constants are $pK_{a1}=3.98$, $pK_{a2}=4.62$, and $pK_{a3}=5.17$. By using the difference in pK_a values, the carboxyl groups on the diglucuronic unit were selectively protected by acetyl groups, as shown in Scheme 2, whereas the one on the triterpenoid backbone was conjugated with *trans*-azodianiline (*trans*-Azo) by an amidation reaction to give the intermediate *trans*-GAGP. After hydrolysis under basic conditions, resin was used to remove the ions and afford *trans*-GAG due to its high polarity. This selective protection of the carboxyl groups provides a convenient way to synthesize other GA derivatives.

As a general procedure, *trans*-GAG was initially dispersed and heated in different solvents, then subsequently cooled to room temperature. After standing for 20 min, the bottle-inversion method^[15] was used to determine whether a supramolecular gel had formed or not. As illustrated in Table S1 and Figure S1, only precipitates or clear solutions were formed in deionized (DI) water (Table S1, entry 1), Tris-HCl (Table S1, entries 2–6), phosphate buffer saline (PBS; Table S1, entries 7–8), Kphos (Table S1, entries 9–10), and Naphos buffer (Table S1, entries 11–13), regardless of the buffer concentration or pH (1–100 mM, pH 6–8). Additionally, different mixed solvents were also tested. As can be seen, *trans*-GAG formed a transparent gel and a partial gel in DMSO/H₂O and MeOH/H₂O, respectively (Table S1, entries 14–15), but only clear solutions in other systems (Table S1, entries 16–21).

To optimize the gelation conditions, the gelation ability of *trans*-GAG in DMSO/H₂O and MeOH/H₂O with different volume ratios was further tested. As shown in Table 1 and Figure 1, stable gels were obtained with DMSO/H₂O at a volume ratio of 2:8 (Table 1, entry 3), and with MeOH/H₂O at ratios of 3:7, 4:6, and 5:5 (Table 1, entries 7–9). An increase in either water or organic phase content resulted in collapse of the gel on account of the hydrophilic/hydrophobic balance (Table 1, entries 1–2,



Scheme 2. Synthetic route of *trans*-GAG.

Table 1. Gelation results for *trans*-GAG in DMSO/H₂O and MeOH/H₂O at different volume ratios.

Entry	Solvent	Ratio	State ^[a]	MGC [mg mL ⁻¹] ^[b]
1	DMSO/H ₂ O	1:10	P	–
2	DMSO/H ₂ O	1:9	PG	–
3	DMSO/H ₂ O	2:8	G	17.6
4	DMSO/H ₂ O	3:7	S	–
5	MeOH/H ₂ O	1:9	P	–
6	MeOH/H ₂ O	2:8	PG	–
7	MeOH/H ₂ O	3:7	G	13.9
8	MeOH/H ₂ O	4:6	G	16.1
9	MeOH/H ₂ O	5:5	G	28.2
10	MeOH/H ₂ O	6:4	P	–

[a] G = gel, PG = partial gel; P = precipitate, S = solution. [b] MGC = minimum gelation concentration at RT.

4–6, and 10). Therefore, DMSO/H₂O (2:8, v/v) was chosen as the solvent in the following study.

To clarify the driving forces during the gelation process, UV/Vis and ¹H NMR spectroscopy experiments were performed. As shown in Figure S2, *trans*-GAG in DMSO exhibited a broad band that ranged from $\lambda=250$ to 500 nm with maxima centered at $\lambda=262$ and 378 nm, which were attributed to the π - π^* transition of GA and the *trans*-Azo moiety, respectively. Upon addition of water, a blueshift of 10 nm in the absorption maximum was observed, which was mainly due to the forma-

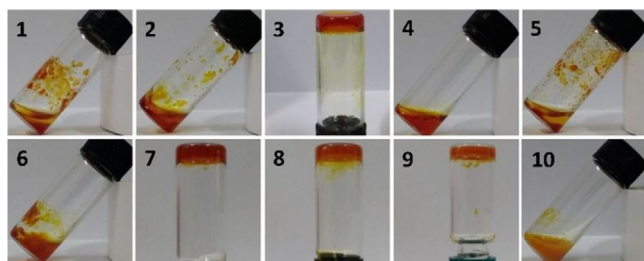


Figure 1. Photographs of the gelation results of *trans*-GAG in DMSO/H₂O and MeOH/H₂O at different volume ratios (the numbers correspond to the entries in Table 1).

tion of H-aggregates primarily driven by π - π stacking.^[15c,16] It was further confirmed by the ¹H NMR spectra (Figure S3), in which the signals of *trans*-GAG became broad compared with those recorded in [D₆]DMSO. Additionally, the resonance of aromatic protons belonging to the *trans*-Azo unit shifted from δ = 7.87 to 7.78 ppm when the water content reached 20% (Table S2), which clearly indicated the existence of π - π stacking.^[3b,4d,17] Additionally, signals for 12-H and methyl protons on the triterpenoid backbone were shifted upfield from δ = 5.46 and 0.71 to 1.39 ppm to δ = 5.38 and 0.64 to 1.26 ppm (Table S2), respectively, which revealed the involvement of hydrophobic effects.^[18] Notably, the signal from the amide proton shifted downfield from δ = 9.59 to 9.61 ppm when the water content reached 10%, and eventually disappeared with a further increase in water because of hydrogen bonding.^[19] Apparently, the synergetic combination of π - π stacking, hydrophobic effect, and hydrogen bonding promotes gel formation.

Upon irradiation with UV light at λ = 365 nm for 30 min, the yellow gel of *trans*-GAG in DMSO/H₂O (2:8 v/v) gradually converted into a sol, as shown in Scheme 1, which strongly implied the collapse of aggregation caused by *trans*-to-*cis* light isomerization of the Azo moiety. Moreover, the resulting sol could become a gel again within 12 h under visible light due to reversible isomerization that promoted the reaggregation of GAG molecules in the *trans* form. This gel-sol transition was evaluated by examining AFM and SEM images. Spheres with a diameter of around 200 to 500 nm were observed in the *trans*-GAG gel (Figure 2a,b), whereas the microscopic structures within the *cis*-GAG sol were converted to irregular aggregates after irradiation with UV light (Figure 2c,d).

The switchable conformation behavior of *trans*-GAG was further investigated by examining the UV/Vis spectra. As shown in Figure 3a, *trans*-GAG displayed an absorption peak at λ = 371 nm, which was attributed to the π - π^* transition of the *trans*-Azo unit.^[4b,16a,20] After irradiation with UV light at λ = 365 nm, the band at λ = 371 nm decreased from 0.84 to 0.45 within 140 s until it reached a plateau, accompanied by a slight increase at λ = 470 nm, which was attributed to the n - π^* transition of the *cis*-Azo moiety.^[3c] This strongly indicated that *trans*-GAG underwent a change in conformation to *cis*-GAG, and that dynamic equilibrium was attained within 140 s. Conversely, the isomerization from *cis*-GAG to *trans*-GAG proceeded relatively faster under visible light, and needed only 80 s to recover from 0.45 to 0.84 (Figure 3b). Moreover, under alternat-

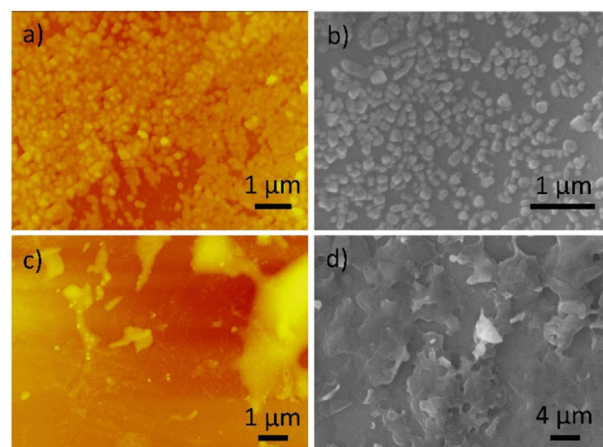


Figure 2. AFM and SEM images of a,b) *trans*-GAG gel and c,d) *cis*-GAG sol in DMSO/H₂O (2:8 v/v) at a concentration of 14 mM.

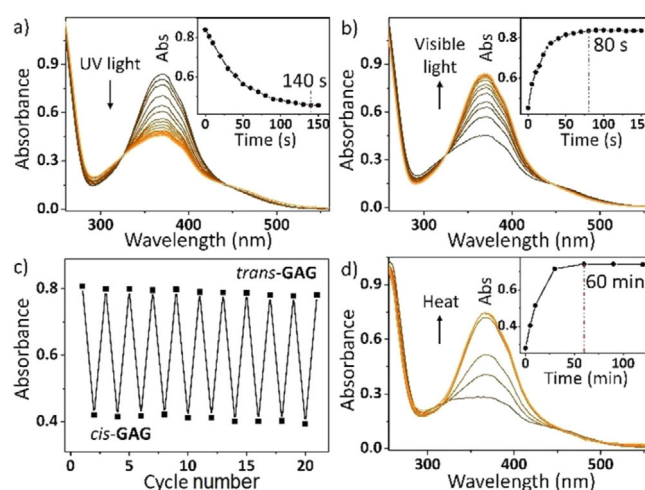


Figure 3. Conformation conversion of GAG (0.04 mM) in DMSO/H₂O (2:8 v/v) a) from *trans* to *cis* by irradiation with UV light (λ = 365 nm, 12 W) and b) from *cis* to *trans* by irradiation with visible light (40 W). c) Conversion cycle test of *cis*-GAG/*trans*-GAG under alternated UV and visible light for 3 min. d) Conformation conversion from *cis*-GAG to *trans*-GAG after heating at 80 °C.

ing irradiation with UV and visible light, this cycle could be repeated multiple times with no macroscopic retrogression (Figure 3c). In addition, the transition between *trans*- and *cis*-GAG could also be realized by heating.^[1d,21] As shown in Figure 3d, the continuous heating of *cis*-GAG at 80 °C for 60 min resulted in conversion to *trans*-GAG with absorption values from 0.28 to 0.74. Notably, this conversion was much slower than the one observed with visible-light irradiation. Similar to the results in Figure 3c, the reversible change between *cis*-GAG and *trans*-GAG induced by UV light or heat could be repeated numerous times (Figure S4). Given the above, the symmetrical GAG molecule could reversibly convert between *cis* and *trans* conformations under either visible/UV light, or heat/UV light conditions.

To obtain a better insight into the reversible conformation of GAG, ¹H NMR spectroscopy experiments as a function of illumination time were performed. As illustrated in Figure 4 and

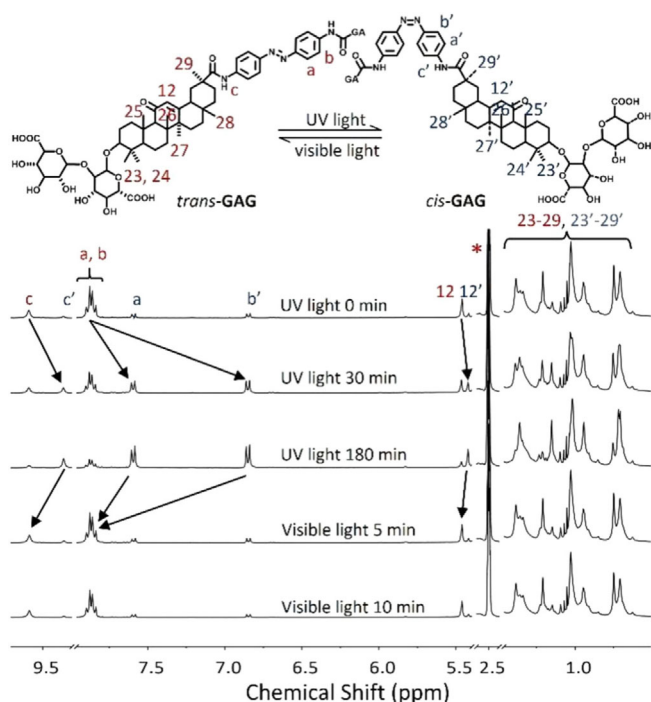


Figure 4. ^1H NMR spectra of **GAG** upon irradiation with UV light (12 W) and visible light (40 W) for different time periods (6.40 mm, * indicates $[\text{D}_2\text{O}]_{\text{DMSO}}$).

Table S3, initially a mixture of 82% *trans*-**GAG** and 18% *cis*-**GAG** was observed. Upon irradiation at $\lambda = 365$ nm, the proton integrations of the Azo unit at $\delta = 7.87$ ppm (a-H, b-H), amide at $\delta = 9.59$ ppm (c-H), and triterpenoid aglycon at around $\delta = 5.46$ and 0.71 to 1.39 ppm (12-H, 23-H–29-H) in *trans*-**GAG** gradually declined, whereas those of the corresponding protons in *cis*-**GAG** (a'-H, b'-H, c'-H, 12'-H, 23'-H–29'-H) increased. Eventually the spectrum reached a photostationary state after 180 min and revealed around 23% *trans*-**GAG** and 77% *cis*-**GAG**, which clearly indicated the conversion from *trans* to *cis* conformation. It should be noted that, due to the concentrated solution used in the NMR spectroscopy experiment, more time was needed to reach the photostationary state compared with the one in UV/Vis measurement. Similar to the results in Figure 3, a shorter time (only 5 min) was required when *cis*-**GAG** reverted to its original level under visible light. It was apparent that **GAG** could reversibly transform between *cis* and *trans* conformation under alternating UV and visible light.

Rheological studies provide direct information on the viscoelastic behavior of soft materials. Normally, the storage modulus (G') describes the ability of deformed materials to store energy, and the loss modulus (G'') corresponds to the ability to dissipate energy. The G' and G'' values as a function of angular frequency for *trans*-**GAG** before and after the exposure to UV light are shown in Figure 5a. Before UV irradiation, the G' value was greater than the respective G'' value, and invariant to the frequency under an applied strain of 1% in the frequency range of 0.5 to 100 rad s^{-1} , which revealed the viscoelastic nature of the *trans*-**GAG** gel over the entire frequency range.^[15b,22] After irradiating the gel for 30 min, a decrease in

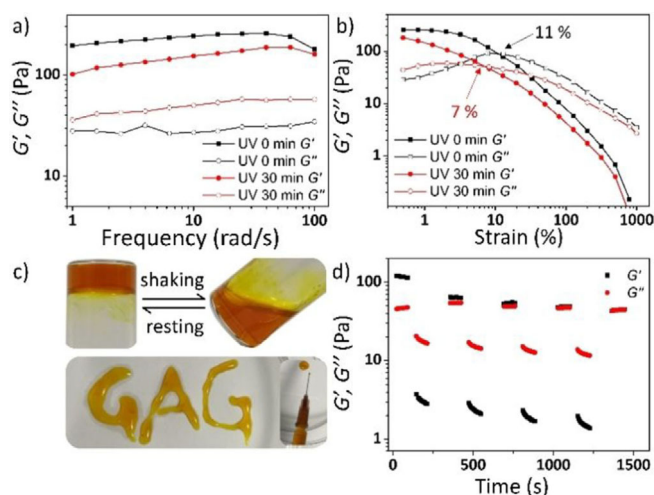


Figure 5. a) Oscillatory frequency and b) amplitude sweep of *trans*-**GAG** gel on exposure to UV light for 0 and 30 min. c) Digital photos of the sol–gel transition between shaking and resting, and the injection ability of the gel. d) Oscillatory time sweep for the *trans*-**GAG** gel under alternating step strains of 1 and 70% (26 °C). Concentration 20 mg mL^{-1} (DMSO/ H_2O 2:8 v/v).

the value of G' from 220 to 150 Pa was observed, which revealed that a low viscosity and a fast relaxation process were produced. Furthermore, the critical point (crossing point of G' and G'') shifted from 11% to a low strain value of 7% under an applied frequency of 10 rad s^{-1} as the irradiation time progressed (Figure 5b), which further confirmed that rheological properties of the **GAG** gel relied heavily on the percentage of *trans*-**GAG** and *cis*-**GAG** in the material.

It should be noted that after conversion into a sol by shaking, the *trans*-**GAG** gel turned back into a robust gel after resting (Figure 5c). This self-healing behavior was verified by the alternate step strain test. According to the results in Figure 5b, alternating 1 and 70% strains were applied with the frequency fixed at 10 rad s^{-1} . As shown in Figure 5d, initially a 1% strain was applied to *trans*-**GAG** gel, for which G' showed a higher value than G'' , which revealed the distinct gel characteristics. Subsequently, a 70% strain was applied, which resulted in a drastic decrease in the value of G' to below G'' , indicating that the gel behavior was destroyed and the sol behavior was prominent. After removing the high strain and applying a constant strain of 1% again, the original mechanical strength of the *trans*-**GAG** gel was almost recovered. Clearly, the large strain (70%) destroyed the microstructure of the *trans*-**GAG** gel and thus resulted in gel collapse and a drastic decrease in the G' value, whereas a small strain (1%) exerted a force to help the remixing of *trans*-**GAG** molecules and, therefore, refabricated the inner network of the gel. These results strongly indicated the self-healing property of the *trans*-**GAG** gel, and made it suitable as an injectable material. As shown in Figure 5c, *trans*-**GAG** gel could easily be transferred into a syringe and extruded to create desired patterns on the substrate, which may enable it to create desired structures by 3D printing.

Furthermore, the cell viability of *trans*-**GAG** was investigated by co-culturing with the breast cancer cell line MCF-7. On account of the natural origin of **GA**, *trans*-**GAG** displayed out-

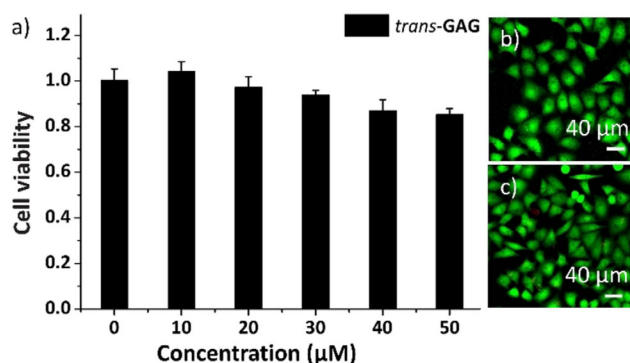


Figure 6. a) Cell viability and cell images after treatment b) without and c) with *trans*-GAG for 24 h. Cells were stained with fluorescein diacetate (FDA, green) and propidium iodide (PI, red).

standing biocompatibility even at concentrations of up to 50 μM, as determined by using a CellTiter-Blue™ assay (Promega; Figure 6a). As shown in Figure 6b,c, live cells were stained green and dead cells were stained with red, which indicated that the majority of MCF-7 cells survived in the presence of *trans*-GAG (50 μM) for 24 h. However, cell viability and morphology were the only parameters examined in this study as preliminary indicators of the suitability of *trans*-GAG gel for tissue-engineering applications. Future studies will include the construction of cell-contained self-healing multilayer structures in hybrid tissue engineering.

Conclusions

In summary, a symmetrical glycyrrhizic acid functionalized azobenzene gelator, *trans*-GAG, was synthesized and could form stable gels in MeOH/H₂O and DMSO/H₂O, mainly promoted by the synergistic effects of hydrogen bonding, π-π stacking, and hydrophobic forces. Moreover, this gel exhibited a typical light-responsive behavior, that is, a reversible gel-sol transition occurred upon irradiation with alternating UV and visible light, due to a *cis*-GAG/*trans*-GAG isomerization that could be confirmed by using UV/Vis spectroscopy, NMR spectroscopy, morphology, and rheology studies. Furthermore, the *trans*-GAG gel displayed a distinct injectable self-healing property and outstanding biocompatibility, which gives the *trans*-GAG gel potential applications in 3D printing. This work provides a simple yet rational strategy to fabricate stimuli-responsive materials from naturally occurring eco-friendly molecules.

Experimental Section

General materials

Glycyrrhizic acid (GA) was purchased from J&K Chemical. *N*-(3-dimethylaminopropyl)-*N'*-ethylcarbodiimide hydrochloride (EDC), potassium dioxide, *p*-phenylenediamine, and 4-dimethylaminopyridine (DMAP) were purchased from Aladdin. Other common chemicals were from local commercial suppliers.

Characterization

¹H and ¹³C NMR spectra were recorded in [D₆]DMSO or D₂O at 25 °C by using a JEOL JNM-ECA 400 spectrometer. Electrospray ionization mass spectroscopy (ESI-MS) was performed by using a Bruker ESQUIRE-LC spectrometer in positive mode. Matrix-assisted laser desorption/ionization- time of flight-mass spectrometry (MALDI-TOF-MS) was performed by using an AXIMA-Performance in positive mode. UV/Vis spectra were measured by using a Thermo Scientific Nanodrop 2000C spectrophotometer. Scanning electron microscopy (SEM) was recorded by using a Hitachi S-4800 microscope operated at 10–15 kV. Atomic force microscopy (AFM) measurements were performed by using a NanoScope 3D AFM (Veeco, USA) in the tapping mode with a SiN₄ tip (radius 10–20 nm). Rheological experiments were performed in a plate geometry (diameter 25 mm) on the rheometer plate by using a TA Instrument.

Cell viability

The breast cancer cell line MCF-7 was provided by Norman Bethune Health Science Center, Jilin University, and grown in Dulbecco's modified Eagle's medium (DMEM) supplemented with 10% fetal bovine serum (FBS) in an atmosphere of 5% CO₂ at 37 °C. Cells were seeded in a 96-well culture plate with a density of 1 × 10⁵. After overnight incubation, the medium was replaced with fresh DMEM that contained *trans*-GAG at different concentrations and the plates were incubated for another 24 h. Next, CellTiter-Blue reagent (20 μL) was added to each well and the cells were incubated for a further 3 h to perform the cell viability assay. The fluorescence intensity was measured at λ = 560/590 nm (E_x/E_m) by using a BioTek Synergy H1 microplate reader.

Cell imaging

MCF-7 cells were seeded in 24-well culture plate with a seeding density of 4 × 10⁴. After overnight incubation, cells were treated with DMEM that contained 50 μM *trans*-GAG and then co-cultured at 37 °C. After 24 h, the samples were stained with a solution of FDA (5 μg mL⁻¹) and PI (10 μg mL⁻¹). Cells were imaged by using an LSM 700 confocal laser scanning microscope imaging system (Carl Zeiss). FDA was excited by using a λ = 488 nm laser to emit λ = 500–600 nm fluorescence, and PI was excited by using a λ = 555 nm laser to emit λ = 560–700 nm fluorescence.

Synthesis of *trans*-4,4'-azodianiline (*trans*-Azo)^[9a]

Potassium superoxide (11.84 g, 166.45 mmol) and *p*-phenylenediamine (4.50 g, 41.61 mmol) were dispersed in anhydrous tetrahydrofuran (180 mL) and degassed with high-purity nitrogen for 3 min. After heating at reflux for 24 h, the mixture was filtered and the filtrate was evaporated to remove the solvent. The crude product was purified by using silica column chromatography (dichloromethane/ethyl acetate 80:1 v/v) to afford *trans*-Azo as a crimson powder (0.62 g, yield 15%). ¹H NMR (400 MHz, [D₆]DMSO): δ = 7.52 (d, *J* = 8.0 Hz, 4H; Ph-H), 6.62 (d, *J* = 8.0 Hz, 4H; Ph-H), 5.74 ppm (s, 4H; -NH₂); ¹³C NMR (100 MHz, [D₆]DMSO): δ = 151.0, 143.1, 123.8, 113.4 ppm; ESI-MS (+): *m/z*: 213 [M+H]⁺, 254 [M+CH₃CN+H]⁺.

Synthesis of acetyl- and methoxyl-protected glycyrrhizic acid (GAP)^[23]

A solution of GA (10.00 g, 12.15 mmol) in methanolic HCl (2 wt %, 360 mL) was stirred at RT for 10 h, and then an appropriate amount of triethylamine was added to tune the pH to 7. After re-

removal of the solvents, the intermediate was dissolved in a mixture of pyridine and acetic anhydride (1:1 v/v, 300 mL), and the reaction solution was stirred at RT for 36 h. Then the mixture was poured slowly into ice water and the precipitate was filtered. The crude product was further purified by using silica column chromatography (dichloromethane/methanol 80:1 v/v) to give **GAP** as a white solid (5.27 g, yield 41%). ¹H NMR (400 MHz, [D₆]DMSO): δ = 0.75 (s, 3H; 28-CH₃), 0.76 (s, 3H; 24-CH₃), 0.98 (s, 3H; 23-CH₃), 1.04 (s, 2 × 3H; 25, 26-CH₃), 1.10 (s, 3H; 29-CH₃), 1.35 (s, 3H; 27-CH₃), 1.91, 1.94, 1.95, 1.96, 2.11 (s, 5 × 3H; OCCH₃), 2.33 (s, 1H; 9-H), 3.06 (dd, J₁ = 12.0 Hz, J₂ = 4.0 Hz, 1H; 3-H), 3.62 (s, 2 × 3H; OCH₃), 3.67 (t, J = 8.0 Hz, 1H; 5'-H), 4.38 (t, J = 8.0 Hz, 1H; 5''-H), 4.54 (d, J = 12.0 Hz, 1H; 1'-H), 4.67 (t, J = 10.0 Hz, 1H; 2''-H), 4.76 (d, J = 4.0 Hz, 1H; 2'-H), 4.86 (t, J = 10.0 Hz, 1H; 4'-H), 4.93 (t, J = 10.0 Hz, 1H; 4''-H), 4.99 (d, J = 8.0 Hz, 1H; 3'-H), 5.24 (t, J = 8.0 Hz, 1H; 3''-H), 5.32 (t, J = 10.0 Hz, 1H; 1''-H), 5.40 (s, 1H; 12-H), 12.18 ppm (s, 1H; COOH); ¹³C NMR (100 MHz, [D₆]DMSO): δ = 199.0, 169.80, 169.76, 169.5, 169.3, 169.1, 167.7, 166.9, 127.3, 102.0, 99.3, 89.4, 76.5, 73.0, 71.7, 71.1, 70.9, 70.7, 69.4, 69.2, 61.0, 54.2, 52.4, 48.0, 44.9, 43.1, 42.9, 40.7, 37.5, 36.3, 32.1, 31.5, 28.4, 27.9, 27.0, 26.1, 25.8, 25.4, 23.0, 20.6, 20.2, 20.1, 18.3, 16.9, 16.2, 15.6 ppm; ESI-MS (+): m/z: 1062 [M+H]⁺, 1079 [M+NH₄]⁺.

Synthesis of *N,N'*-(azobenzene-4,4'-diyl)-diprotected glycyrrhizic amide (*trans*-GAGP)

trans-Azo (0.33 g, 1.57 mmol) was added to a solution of **GAP** (5.00 g, 4.71 mmol), EDC (0.96 g, 5.03 mmol), and DMAP (0.61 g, 5.03 mmol) in chloroform (55 mL), and the mixture was heated at reflux for 62 h. After removal of the solvent, the crude product was dispersed by water with ultrasonication for 10 min, then the precipitate was collected and redissolved in dichloromethane. The organic phase was washed with water and brine, and then dried over Na₂SO₄. After evaporation of the solvent, the crude product was purified by using silica column chromatography (dichloromethane/methanol 80:1 v/v) to afford **GAGP** as a brown solid (2.20 g, yield 61%). ¹H NMR (400 MHz, [D₆]DMSO): δ = 0.75 (s, 2 × 2 × 3H; 24, 28-CH₃), 0.98 (s, 2 × 3H; 23-CH₃), 1.04 (s, 2 × 2 × 3H; 25, 26-CH₃), 1.21 (s, 2 × 3H; 29-CH₃), 1.40 (s, 2 × 3H; 27-CH₃), 1.92, 1.94, 1.95, 1.96, 2.12 (s, 2 × 5 × 3H; OCCH₃), 2.35 (s, 2 × 1H; 9-H), 3.05 (dd, J₁ = 4.0 Hz, J₂ = 4.0 Hz, 2 × 1H; 3-H), 3.62 (s, 2 × 2 × 3H; OCH₃), 3.68 (t, J = 8.0 Hz, 2 × 1H; 5'-H), 4.39 (d, J = 8.0 Hz, 2 × 1H; 5''-H), 4.54 (d, J = 8.0 Hz, 2 × 1H; 1'-H), 4.67 (t, J = 10.0 Hz, 2 × 1H; 2''-H), 4.76 (d, J = 8.0 Hz, 2 × 1H; 2'-H), 4.86 (t, J = 10.0 Hz, 2 × 1H; 4'-H), 4.93 (t, J = 10.0 Hz, 2 × 1H; 4''-H), 5.00 (d, J = 8.0 Hz, 2 × 1H; 3'-H), 5.25 (t, J = 10.0 Hz, 2 × 1H; 3''-H), 5.33 (t, J = 10.0 Hz, 2 × 1H; 1''-H), 5.47 (s, 2 × 1H; 12-H), 7.87 (m, 8H; Azo-H), 9.59 ppm (s, 2 × 1H; CONH); ¹³C NMR (100 MHz, [D₆]DMSO): δ = 199.0, 174.9, 169.8, 169.6, 169.5, 169.3, 169.1, 167.7, 166.9, 147.7, 142.1, 127.5, 123.1, 120.4, 102.1, 99.5, 99.3, 89.4, 76.5, 73.0, 71.7, 71.1, 70.9, 70.7, 69.4, 69.2, 61.1, 54.2, 52.4, 47.9, 44.9, 44.3, 43.0, 36.3, 31.6, 28.3, 27.9, 27.0, 22.9, 20.6, 20.3, 20.1, 18.3, 16.2, 15.6 ppm; MALDI-TOF-MS (+): m/z calcd for C₁₂₀H₁₆₀N₄O₄₀: 2321.0642; found: 2321.2606 [M+Na]⁺.

Synthesis of *N,N'*-(azobenzene-4,4'-diyl)-diglycyrrhizic amide (*trans*-GAG)

GAGP (2.80 g, 1.22 mmol) was added to a solution of KOH (5 wt%) in water and ethanol (1:1 v/v, 50 mL), and the reaction mixture was stirred at RT for 30 h. The mixture was poured into resin that had been activated and stirred for another 20 h at RT. Next, the resin was filtered and washed with methanol (80 mL), and the filtrates were combined. After removal of the methanol and ethanol, the solution was lyophilized to afford **GAG** as a deep-yellow powder

(2.20 g, yield 95%). ¹H NMR (400 MHz, [D₆]DMSO): δ = 0.71 (s, 2 × 3H; 24-CH₃), 0.75 (s, 2 × 3H; 28-CH₃), 0.95 (s, 2 × 3H; 23-CH₃), 1.03 (s, 2 × 2 × 3H; 25, 26-CH₃), 1.21 (s, 2 × 3H; 29-CH₃), 1.39 (s, 2 × 3H; 27-CH₃), 2.34 (s, 2 × 1H; 9-H), 3.56 (d, J = 8.0 Hz, 2 × 1H; 5'-H), 3.64 (d, J = 8.0 Hz, 2 × 1H; 5''-H), 4.41 (d, J = 8.0 Hz, 2 × 1H; 1''-H), 4.50 (d, J = 4.0 Hz, 2 × 1H; 1'-H), 5.46 (s, 2 × 1H; 12-H), 7.87 (m, 8H; Azo-H), 9.58 (s, 2 × 1H; CONH), 12.60 ppm (s, 2 × 2 × 1H; COOH); ¹³C NMR (100 MHz, [D₆]DMSO): δ = 198.9, 174.9, 170.1, 169.9, 169.5, 147.7, 142.0, 127.5, 123.1, 120.4, 104.7, 103.5, 88.2, 82.6, 76.2, 75.8, 75.6, 75.2, 74.8, 71.5, 71.2, 61.1, 54.3, 47.9, 44.8, 44.2, 42.9, 40.6, 38.5, 36.3, 32.1, 31.5, 30.4, 28.3, 27.9, 27.1, 26.1, 25.9, 25.7, 22.9, 18.6, 18.3, 16.2, 15.9 ppm; ESI-MS (+): m/z: 1845 [M+Na]⁺.

Acknowledgements

This work is supported by National Key R&D program of China (no. 2017YFD0200302), the NSFC (no. 21604085), the Jilin Science Foundation for Youths (no. 20160520135JH), and the Fundamental Research Funds for the Central Universities (ZY1831). J.H. thanks the State Key Laboratory of Polymer Physics and Chemistry, CIAC, for support.

Conflict of interest

The authors declare no conflict of interest.

Keywords: azo compounds · gels · glycyrrhizic acid · self-assembly · terpenoids

- [1] a) X. Yu, L. Chen, M. Zhang, T. Yi, *Chem. Soc. Rev.* **2014**, *43*, 5346–5371; b) B. G. Bag, R. Majumdar, S. K. Dinda, P. P. Dey, G. C. Maity, V. A. Mallia, R. G. Weiss, *Langmuir* **2013**, *29*, 1766–1778; c) R. Yang, S. Peng, W. Wan, T. C. Hughes, *J. Mater. Chem. C* **2014**, *2*, 9122–9131; d) W. Zhang, Y. Chen, J. Yu, X. J. Zhang, Y. Liu, *Chem. Commun.* **2016**, *52*, 14274–14277.
- [2] a) H. Xie, M. Asad Ayoubi, W. Lu, J. Wang, J. Huang, W. Wang, *Sci. Rep.* **2017**, *7*, 8459; b) H. N. Joo, T. Van Thi Nguyen, H. K. Chae, Y. J. Seo, *Bioorg. Med. Chem. Lett.* **2017**, *27*, 2415–2419; c) G. F. Liu, W. Ji, C. L. Feng, *Langmuir* **2015**, *31*, 7122–7128.
- [3] a) T. Naota, H. Koori, *J. Am. Chem. Soc.* **2005**, *127*, 9324–9325; b) Z. X. Liu, Y. Feng, Z. C. Yan, Y. M. He, C. Y. Liu, Q. H. Fan, *Chem. Mater.* **2012**, *24*, 3751–3757; c) P. Fatás, J. Bachl, S. Oehm, A. I. Jimenez, C. Catiuela, D. Diaz Diaz, *Chem. Eur. J.* **2013**, *19*, 8861–8874.
- [4] a) X. Gu, B. Bai, H. Wang, M. Li, *RSC Adv.* **2017**, *7*, 218–223; b) L. Shi, X. Ran, Y. Li, Q. Li, W. Qiu, L. Guo, *RSC Adv.* **2015**, *5*, 38283–38289; c) W. A. Velema, M. C. A. Stuart, W. Szymanski, B. L. Feringa, *Chem. Commun.* **2013**, *49*, 5001–5003; d) Z. Li, Y. Huang, D. Fan, H. Li, S. Liu, L. Wang, *Front. Chem. Sci. Eng.* **2016**, *10*, 552–561.
- [5] a) Y. Y. Ren, Z. Xu, G. Li, J. Huang, X. Fan, L. Xu, *Dalton Trans.* **2017**, *46*, 333–337; b) J. Li, I. Cvrtila, M. Colomb-Delsuc, E. Otten, S. Otto, *Chem. Eur. J.* **2014**, *20*, 15709–15714.
- [6] a) Z. M. Yang, H. W. Gu, D. G. Fu, P. Gao, K. J. K. Lam, B. Xu, *Adv. Mater.* **2004**, *16*, 1440–1444; b) J. Fan, R. Li, H. Wang, X. He, T. P. Nguyen, R. A. Letteri, J. Zou, K. L. Wooley, *Org. Biomol. Chem.* **2017**, *15*, 5145–5154.
- [7] a) Y. Gao, J. Hao, J. Wu, X. Zhang, J. Hu, Y. Ju, *Langmuir* **2016**, *32*, 1685–1692; b) F. M. Menger, A. V. Peresypkin, *J. Am. Chem. Soc.* **2003**, *125*, 5340–5345.
- [8] a) X. Cao, X. Liu, L. Chen, Y. Mao, H. Lan, T. Yi, *J. Colloid Interface Sci.* **2015**, *458*, 187–193; b) R. Yang, S. Peng, T. C. Hughes, *Soft Matter* **2014**, *10*, 2188–2196; c) M. Mrinalini, N. Vamsi Krishna, J. V. S. Krishna, S. Prasanthkumar, L. Giribabu, *Phys. Chem. Chem. Phys.* **2017**, *19*, 26535–26539.
- [9] a) H. Sun, L. Zhao, T. Wang, G. An, S. Fu, X. Li, X. Deng, J. Liu, *Chem. Commun.* **2016**, *52*, 6001–6004; b) J. H. Kim, M. Seo, Y. J. Kim, S. Y. Kim, *Langmuir* **2009**, *25*, 1761–1766.

- [10] T. M. Doran, D. M. Ryan, B. L. Nilsson, *Polym. Chem.* **2014**, *5*, 241–248.
- [11] M. N. Asl, H. Hosseinzadeh, *Phytother. Res.* **2008**, *22*, 709–724.
- [12] a) S. W. Kim, Y. Jin, J. H. Shin, I. D. Kim, H. K. Lee, S. Park, P. L. Han, J. K. Lee, *Neurobiol. Dis.* **2012**, *46*, 147–156; b) C. Y. Wang, T. C. Kao, W. H. Lo, G. C. Yen, *J. Agric. Food Chem.* **2011**, *59*, 7726–7733; c) Y. A. Yang, W. J. Tang, X. Zhang, J. W. Yuan, X. H. Liu, H. L. Zhu, *Molecules* **2014**, *19*, 6368–6381; d) L. A. Baltina, R. M. Koudratenko, J. L. A. Baltina, O. A. Plyasunova, A. G. Pokrovskii, G. A. Tolstikov, *Pharm. Chem. J.* **2009**, *43*, 539–548; e) S. Schmidt, K. Heymann, M. F. Melzig, S. Bereswill, M. M. Heimesaat, *Planta. Med.* **2016**, *82*, 1540–1545.
- [13] A. Saha, J. Adamcik, S. Bolisetty, S. Handschin, R. Mezzenga, *Angew. Chem. Int. Ed.* **2015**, *54*, 5408–5412; *Angew. Chem.* **2015**, *127*, 5498–5502.
- [14] a) Z. Wan, Y. Sun, L. Ma, J. Guo, J. Wang, S. Yin, X. Yang, *Food Funct.* **2017**, *8*, 75–85; b) Z. Wan, Y. Sun, L. Ma, X. Yang, J. Guo, S. Yin, *J. Agric. Food Chem.* **2017**, *65*, 2394–2405; c) L. Ma, Z. Wan, X. Yang, *J. Agric. Food Chem.* **2017**, *65*, 9735–9743.
- [15] a) Y. Zhang, P. Xue, B. Yao, J. Sun, *New J. Chem.* **2014**, *38*, 5747–5753; b) L. Gao, Y. Gao, Y. Lin, Y. Ju, S. Yang, J. Hu, *Chem. Asian J.* **2016**, *11*, 3430–3435; c) P. Choudhury, D. Mandal, S. Brahmachari, P. K. Das, *Chem. Eur. J.* **2016**, *22*, 5160–5172.
- [16] a) G. Narayan, N. S. S. Kumar, S. Paul, O. Srinivas, N. Jayaraman, S. Das, *J. Photochem. Photobiol. A* **2007**, *189*, 405–413; b) L. Lu, T. Hu, Z. Xu, *Spectrochim. Acta Part A* **2017**, *185*, 85–92; c) B. V. Shankar, A. Patnaik, *Langmuir* **2006**, *22*, 4758–4765.
- [17] a) S. J. Lee, S. S. Lee, J. S. Kim, J. Y. Lee, J. H. Jung, *Chem. Mater.* **2005**, *17*, 6517–6520; b) H. L. Fu, C. Po, S. Y. Leung, V. W. Yam, *ACS Appl. Mater. Interfaces* **2017**, *9*, 2786–2795.
- [18] L. Wang, X. Shi, Y. Wu, J. Zhang, Y. Zhu, J. Wang, *Soft Matter* **2018**, *14*, 566–573.
- [19] a) F. Allix, P. Curcio, Q. N. Pham, G. Pickaert, B. Jamart-Grégoire, *Langmuir* **2010**, *26*, 16818–16827; b) P. Goutam, A. Banerjee, *J. Phys. Chem. B* **2008**, *112*, 10107–10115.
- [20] Y. Ogawa, C. Yoshiyama, T. Kitaoka, *Langmuir* **2012**, *28*, 4404–4412.
- [21] L. Vetráková, V. Ladanyi, J. Al Anshori, P. Dvorak, J. Wirz, D. Heger, *Photochem. Photobiol. Sci.* **2017**, *16*, 1749–1756.
- [22] a) S. Bhattacharjee, S. Bhattacharya, *J. Mater. Chem. A* **2014**, *2*, 17889–17898; b) Z. Zhang, S. Zhang, J. Zhang, L. Zhu, D. Qu, *Tetrahedron* **2017**, *73*, 4891–4895.
- [23] D. Du, J. Yan, J. Ren, H. Lv, Y. Li, S. Xu, Y. Wang, S. Ma, J. Qu, W. Tang, Z. Hu, S. Yu, *J. Med. Chem.* **2013**, *56*, 97–108.

Manuscript received: February 1, 2018

Accepted manuscript online: March 5, 2018

Version of record online: ■■■■■ 0000

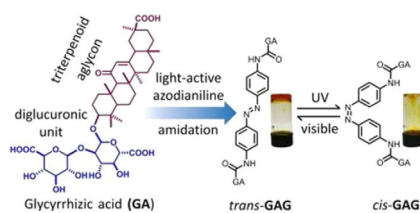
FULL PAPER

Sol–Gel Processes

Heshu Fang, Xia Zhao, Yuan Lin,
Song Yang,* Jun Hu*



A Natural Glycyrrhizic Acid-Tailored Light-Responsive Gelator



Make light work of gelation: A symmetrical azobenzene-functionalized natural glycyrrhizic acid (*trans*-GAG; see figure) was synthesized, and could form a stable light-responsive supramolecular gel due to *cis*–*trans* isomerization. This work provides a simple yet rational way to fabricate functional materials from naturally occurring eco-friendly triterpenes in light of their biocompatibility and biodegradability.